ORIGINAL RESEARCH

Adipocyte-Specific Enhancement of Angiotensin II Type 1 Receptor-Associated Protein Ameliorates Diet-Induced Visceral Obesity and Insulin Resistance

Kengo Azushima, MD, PhD;* Kohji Ohki, MD;* Hiromichi Wakui, MD, PhD; Kazushi Uneda, MD, PhD; Sona Haku, MD; Ryu Kobayashi, MD; Kotaro Haruhara, MD; Sho Kinguchi, MD; Miyuki Matsuda, MSc; Akinobu Maeda, MD, PhD; Yoshiyuki Toya, MD, PhD; Akio Yamashita, PhD; Satoshi Umemura, MD, PhD; Kouichi Tamura, MD, PhD

***Background*—**The renin–angiotensin system has a pivotal role in the pathophysiology of visceral obesity. Angiotensin II type 1 receptor (AT1R) is a major player in the signal transduction of the renin–angiotensin system, and the overactivation of this signaling contributes to the progression of visceral obesity. We have shown that the AT1R-associated protein (ATRAP) promotes AT1R internalization from the cell surface into cytoplasm along with the suppression of overactivation of tissue AT1R signaling. In this study, we examined whether the enhancement of adipose ATRAP expression could efficiently prevent diet-induced visceral obesity and insulin resistance.

***Methods and Results*—**We generated adipocyte-specific ATRAP transgenic mice using a 5.4-kb adiponectin promoter, and transgenic mice and littermate control mice were fed either a low- or high-fat diet for 10 weeks. Although the physiological phenotypes of the transgenic and control mice fed a low-fat diet were comparable, the transgenic mice exhibited significant protection against high-fat diet–induced adiposity, adipocyte hypertrophy, and insulin resistance concomitant with an attenuation of adipose inflammation, macrophage infiltration, and adipokine dysregulation. In addition, when mice were fed a high-fat diet, the adipose expression of glucose transporter type 4 was significantly elevated and the level of adipose phospho-p38 mitogen-activated protein kinase was significantly attenuated in the transgenic mice compared with control mice.

***Conclusions*—**Results presented in this study suggested that the enhancement in adipose ATRAP plays a protective role against the development of diet-induced visceral obesity and insulin resistance through improvement of adipose inflammation and function via the suppression of overactivation of adipose AT1R signaling. Consequently, adipose tissue ATRAP is suggested to be an effective therapeutic target for the treatment of visceral obesity. **(*J Am Heart Assoc*. 2017;6:e004488. DOI: 10.1161/JAHA.116.004488.)**

Key Words: adipocyte • insulin resistance • obesity • receptor • renin–angiotensin system

Visceral obesity causes insulin resistance and promotes hypertension, dyslipidemia, and diabetes mellitus, which in turn results in the development of cardiovascular disease. Increasing trends in the global prevalence of being overweight or obese are now recognized as a major health problem worldwide.[1] The present interventions, however, have not been able to stop the rise in body mass index in most countries, despite the fact that a variety of treatments have been developed, such as bariatric surgery and antiobesity drugs.[2] The lack of effective and tolerable treatments to improve visceral obesity is clearly an unmet medical need.

Visceral obesity is characterized by low-grade inflammation and adipokine dysregulation associated with adipocyte

From the Departments of Medical Science and Cardiorenal Medicine (K.A., K.O., H.W., K.U., S.H., R.K., K.H., S.K., M.M., A.M., Y.T., S.U., K.T.) and Molecular Biology (A.Y.), Yokohama City University Graduate School of Medicine, Yokohama, Japan; Cardiovascular and Metabolic Disorders Program, Duke-NUS Medical School, Singapore (K.A.).

*Dr Azushima and Dr Ohki contributed equally to this work.

Correspondence to: Kouichi Tamura, MD, PhD, FACP, FAHA, or Kengo Azushima, MD, PhD, Department of Medical Science and Cardiorenal Medicine, Yokohama City University Graduate School of Medicine, 3-9 Fukuura, Kanazawa-ku, Yokohama 236-0004, Japan. E-mails: tamukou@med.yokohama-cu.ac.jp, azushima@yokohama-cu.ac.jp

Received August 15, 2016; accepted February 8, 2017.

hypertrophy.[3] The renin–angiotensin system, well recognized for its contribution to the integration and regulation of cardiovascular function, has also been reportedly associated with the development of visceral obesity via its receptor, angiotensin II type 1 receptor (AT1R).[4] Regarding the role of AT1R signaling in adipocytes, it has been reported that adipose dysfunction and inflammation are elicited by the overactivation of this signaling, which in turn contributes to the progression of visceral obesity and insulin resistance in a mouse model.[5] This finding is supported by human studies demonstrating that renin–angiotensin system inhibitors improve glucose metabolism and reduce the incidence of diabetes mellitus in patients with metabolic syndrome.[6,7]

We have shown that AT1R-associated protein (ATRAP; *Agtrap* gene), a molecule that directly interacts with the carboxyl-terminal domain of AT1R, promotes the constitutive internalization of the AT1R from the cell surface into the cytoplasm and suppresses the angiotensin II–mediated overactivation of AT1R signaling.[8–10] Our recent study revealed that systemic ATRAP deficiency exacerbated diet-induced visceral obesity and insulin resistance in mice[11]; however, the mechanism by which ATRAP modulates diet-induced visceral obesity and insulin resistance has not been elucidated, in part because various tissues such as muscle, liver, and adipose tissue exert effects on these phenotypes.

In this current study, we investigated the pathophysiology of adipose tissue ATRAP in the development of visceral obesity by generating transgenic mice overexpressing ATRAP specifically in adipose tissue. To generate transgenic mice, we used a 5.4-kb adiponectin promoter that is reportedly the most effective cassette for conveying adipocyte-specific expression of target genes.[12] These mice exhibited adipocyte-specific ATRAP enhancement and were prevented from diet-induced visceral obesity and insulin resistance concomitant with an attenuation of adipose nicotinamide adenine dinucleotide phosphate (NADPH) oxidase expression and an elevation in adipose glucose transporter type 4 (GLUT4) expression. In addition, the level of adipose phospho-p38 mitogen-activated protein kinase (MAPK), as the downstream signaling pathway of the AT1R, was also attenuated in these transgenic mice. These results suggest that adipose ATRAP enhancement improves diet-induced adipose dysfunction and inflammation via the suppression of overactivation of adipose AT1R signaling. Consequently, adipose tissue ATRAP is suggested to be an effective therapeutic target for the treatment of visceral obesity.

Materials and Methods

This study was performed in accordance with the National Institutes of Health *Guide for the Care and Use of Laboratory Animals*. All animal studies were reviewed and approved by the animal studies committee of Yokohama City University.

Animals and Animal Care

The mice were housed in a controlled environment with a 12-hour light/dark cycle at a temperature of 25°C and were allowed free access to food and water. They were fed either a low-fat diet (LFD; 3.6 kcal/g; 13.3% energy as fat; Oriental Yeast Co, Ltd) or a high-fat diet (HFD; 5.6 kcal/g; 60.0% energy as fat) for 10 weeks beginning at 8 weeks of age, and their body weight and food intake were measured weekly. All experiments in this study were performed with adipocyte-specific ATRAP transgenic mice and their littermate wild-type (WT) mice. At the end of the experimental period (18 weeks of age), mice were anesthetized with an intraperitoneal injection of pentobarbital and then were sacrificed in the fed state between 10 AM and 2 PM. The numbers of mice in each experiment are reported in the tables and figures, as follows: Table 1, n=6 to 10 in each group; Figure 1B, n=3 in each group; Figure 2A through 2E, n=6 to 7 in each group; Figure 3A and 3B, n=2 in each group; Figure 4B, n=6 to 7 in each group; Figure 5A through 5E, n=6 to 7 in each group; Figure 6B, n=6 to 7 in each group; Figure 7A and 7B, n=6 to 10 in each group; Figure 7C through 7F, n=5 to 7 in each group; Figure 8, n=5 to 6 in each group. Figure 9A, n=6 to 9 in each group; Figure 9B, n=6 to 7 in each group; Figure 10A through 10E, n=6 to 10 in each group; Figure 11, n=5 to 8 in each group; Figure 12A and 12B, n=6 to 7 in each group; Figure 13B, n=5 in each group; Figure 13C through 13F, n=5 to 7 in each group.

Generation of Adipocyte-Specific ATRAP Transgenic Mice

Transgenic mice overexpressing ATRAP specifically in adipose tissue were generated on a C57BL/6J background, essentially as described previously with a minor modification.[13–15] Briefly, hemagglutinin-tagged mouse ATRAP cDNA was subcloned into a transgenic vector between the 5.4-kb fragment of the adiponectin promoter (kindly provided by Dr Philipp E. Scherer, The University of Texas Southwestern Medical Center) and the 3′ untranslated region (Figure 1A). This construct was microinjected into the pronucleus of fertilized mouse embryos. Transgenic mice were identified by polymerase chain reaction using forward (TGCTTGGGGCAACTTCACTATC) and reverse (ACGGTGCATGTGGTAGACGAG) primers and were mated with C57BL/6 mice to obtain transgenic mice and their littermate WT mice for the experiments.

Table 1. Body Weight, Tissue Weight, Systolic Blood Pressure, Heart Rate, and Cumulative Food Intake at 18 Weeks in WT and TG Mice on a LFD or HFD

	LFD		HFD	
Variables	WT	TG	WT	TG
Body weight, g	29.8±0.5	29.4±0.4	43.0±1.8‡	36.7±0.7‡§
Epididymal adipose tissue, mg	318±24	298±13	1813±166‡	1189±162‡§
Brown adipose tissue, mg	85±3	84±6	266±23‡	147±9†§
Liver, mg	1288±59	1256±42	1517±191	1195±31
Kidney, mg	169±7	178±8	217±12†	189±9
Systolic blood pressure, mm Hg	114±5	106±5	129±2	124±4*
Heart rate, beat/min	491±28	578±43	671±15‡	725±19†
Cumulative food intake, kcal	850.3±7.3	852.2±12.8	982.1±29.3†	954.0±28.9*

All of the values are the mean±SEM. Data were analyzed by 2-factor ANOVA. n=6 to 10. HFD indicates high-fat diet; LFD, low-fat diet; TG, adipocyte-specific angiotensin II type 1 receptor–associated protein transgenic mice; WT, wild-type mice.
*P<0.05, †P<0.01, ‡P<0.001, vs LFD within the same group.
§P<0.001, vs WT mice on the same diet.

Three-Dimensional Micro–Computed Tomography Analysis

The 3-dimensional micro–computed tomography (3D micro-CT) scan was performed with an in vivo System R_mCT 3-dimensional micro-CT scanner (Rigaku Co.) at the end of the experimental period. Mice were anesthetized using isoflurane and then scanned with 3-dimensional micro-CT. The fat volume was analyzed using CT Atlas Metabolic Analysis v2.03 software (Rigaku Co.).

Histological Analysis

The epididymal white adipose tissue (WAT) and liver were collected and fixed with 10% paraformaldehyde overnight and embedded in paraffin. Tissue sections were stained with hematoxylin and eosin for cell-size determination. WAT paraffin sections were also stained with an antibody against F4/80 (rat monoclonal; Abcam), as described previously.[11] Nonalcoholic fatty liver disease activity score was measured according to the criteria shown in Table 2, as described previously.[16] All images were acquired using a BZ-9000 microscope (Keyence). At least 3 sections for each mouse were analyzed, and the average of these measurements was taken for analysis.

Blood Pressure Measurement by Tail-Cuff Method

Systolic blood pressure and heart rate were measured by the tail-cuff method (MK-2000; Muromachi Kikai Co.) such that the blood pressure was measured without any preheating of the animals, as described previously.[17,18] All measurements were performed between 10 AM and 2 PM. At least 8 measurements were performed in each mouse, and their average was taken for analysis.

Blood Pressure Measurement by Intra-Arterial Catheter Telemetry System

Direct blood pressure measurement in the conscious state was also performed by the radiotelemetric method after HFD feeding, as described previously.[13–15] Briefly, under anesthesia with isoflurane, an incision was made from the chin to the superior sternum, and the left common carotid artery was surgically exposed. A small incision was made in the artery adjacent to the bifurcation, and the tip of a blood pressure transducer (model TA11PA-C10; Data Science International) was placed in the artery. The catheter was then tied, and the transducer was secured in place under the skin of the right flank with tissue adhesive. All skin wounds were closed with 5-0 nylon (Sigma Rex). Ten days after the transplantation, when the circadian rhythm was restored, hemodynamic measurements were recorded every 5 minutes using the Dataquest A.R.T. 4.1 software (Data Science International).

Biochemical Assay

Blood samples were obtained by cardiac puncture when the mice were sacrificed in the fed state. Whole-blood samples were centrifuged at 600g at 4°C for 15 minutes to separate the plasma. The resulting plasma was stored at −80°C until use. Enzymatic assay was used for the determination of the plasma glucose (WAKO Pure Chemical). The plasma insulin concentration was measured with a commercially available ELISA kit (Morinaga Institute of Biological Science, Inc.).

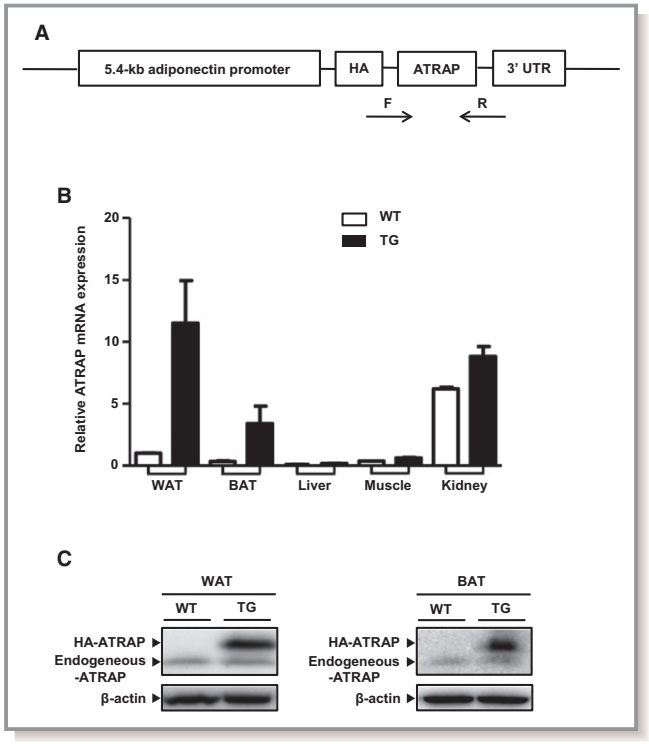

Figure 1. Generation of adipocyte-specific ATRAP transgenic mice. A, Schematic representation of the transgenic vector. F and R indicate the locations of the forward and reverse primers used for the genotyping performed by PCR. B, The relative ATRAP mRNA levels in each tissue (WAT, BAT, liver, muscle, and kidney) analyzed by real-time quantitative reverse transcriptase–PCR (n=3). C, Representative Western blots of ATRAP protein expression in WAT and BAT. ATRAP indicates angiotensin II type 1 receptor–associated protein; BAT, interscapular brown adipose tissue; F, forward; HA, hemagglutinin; PCR, polymerase chain reaction; R, reverse; TG mice, adipocyte-specific ATRAP transgenic mice; UTR, untranslated region; WAT, epididymal white adipose tissue; WT mice, wild-type mice.

Glucose and Insulin Tolerance Tests

The glucose and insulin tolerance tests were performed as described previously, with slight modifications.[11] Briefly, glucose and insulin tolerance tests were performed 4 days apart at the end of the experimental period between 10 AM and 12 PM and between 2 and 4 PM, respectively. For the glucose tolerance test, blood glucose concentrations were measured with a blood glucose test meter (Glutest Neo Super; Sanwa-Kagaku) using blood samples taken from the tail tip of overnight-fasted mice at baseline and at 15, 30, 60 and 120 minutes after the intraperitoneal injection of glucose (1 g/kg body weight). For the insulin tolerance test, insulin (0.75 U/kg body weight in 0.1% BSA; Humulin R-Insulin; Eli Lilly & Co.) was administered via intraperitoneal injection after 4-hour fasting. Blood glucose concentrations were measured at baseline and at 15, 30, 60, and 120 minutes after the injection.

Real-Time Quantitative Reverse Transcriptase–Polymerase Chain Reaction Analysis

Total RNAs were extracted from WAT, interscapular brown adipose tissue (BAT), and liver with ISOGEN (Nippon Gene), and the cDNA was synthesized using the SuperScript III First-Strand System (Invitrogen). Real-time quantitative reverse transcriptase–polymerase chain reaction was performed with an ABI PRISM 7000 Sequence Detection System by incubating the reverse transcription product with TaqMan PCR Master Mix and a designed Taqman probe (Applied Biosystems), essentially as described previously.[13] The mRNA levels were normalized to those of the 18S rRNA control.

Immunoblot Analysis

Western blot analysis was performed as described previously.[19] Briefly, total protein was extracted from WAT with SDS-containing sample buffer, and then the protein concentration of each sample was measured with a DC protein assay kit (Bio-Rad) using BSA as the standard. Equal amounts of protein extract were fractionated on a 5% to 20% polyacrylamide gel (ATTO) and then transferred to a polyvinylidene difluoride membrane using the iBlot Dry Blotting System (Invitrogen). Membranes were blocked for 1 hour at room temperature with phosphate-buffered saline containing 5% skim milk powder and probed overnight at 4°C with specific primary antibodies to GLUT4 (Santa Cruz Biotechnology), Akt, phospho-Akt (Cell Signaling Technology), p38 MAPK (Santa Cruz Biotechnology), phospho-p38 MAPK (Promega Corporation), and ATRAP.[13–15] Next, the membranes were washed and incubated with secondary antibodies for 15 minutes at room temperature. After they were washed, the sites of the antibody–antigen reaction were visualized by enhanced chemiluminescence substrate (Thermo Fisher Scientific). The images were quantitated using a FUJI LAS3000 Image Analyzer (FUJI Film). Regarding the analysis of phospho-Akt, tissues were collected as described previously, with slight modifications.[20] Briefly, after 4-hour fasting, mice were deeply anesthetized with an intraperitoneal injection of pentobarbital. Insulin (5 U/kg body weight in 0.1% BSA; Humulin R-Insulin; Eli Lilly & Co.) was injected through the inferior vena cava, and tissues were quickly collected 2 minutes after the injection.

Statistical Analysis

All data are shown as mean±SEM. Differences were analyzed as follows. A 2-factor ANOVA with a Bonferroni post-test was used to test for differences on the same diet within each genotype or differences in the WT versus transgenic mice (Table 1, Figures 2B, 2D, 2E, 4B, 5A–5E,

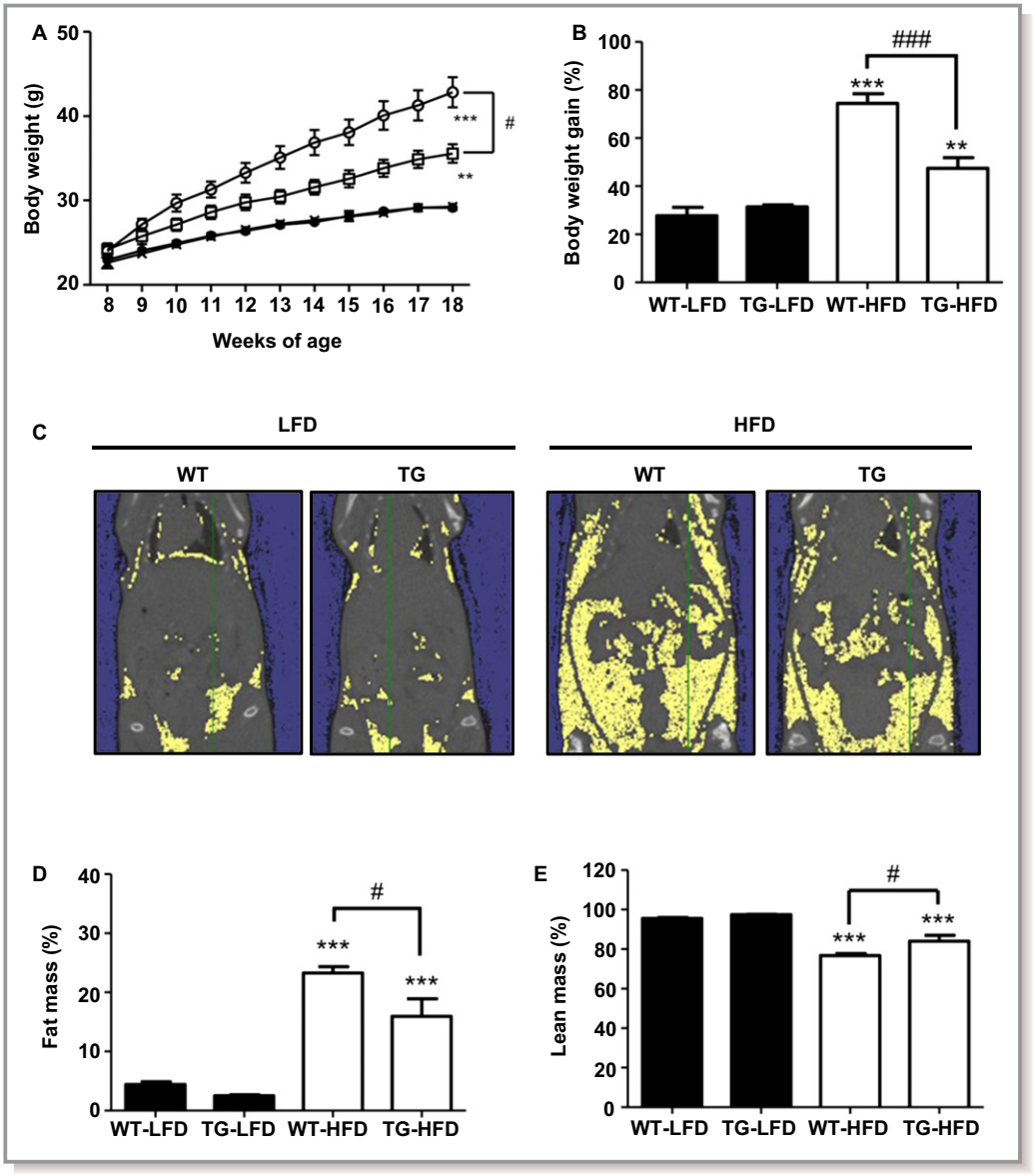

Figure 2. Adipose ATRAP enhancement prevents the increases of body weight and adiposity induced by HFD feeding. A, The change in body weight in WT and TG mice fed an LFD or HFD (n=6 to 7). ●, WT mice fed an LFD; ×, TG mice fed an LFD; ○, WT mice fed an HFD; □, TG mice fed an HFD. $^{**}P<0.01$, $^{***}P<0.001$, vs LFD within the same group. $^{\#}P<0.05$, vs WT mice on the same diet. Data were analyzed by 2-way repeated measures ANOVA. B, Body weight gain of WT and TG mice after 10-week LFD or HFD feeding (n=6 to 7). C, Representative 3D micro-CT images of WT and TG mice after 10-week LFD or HFD feeding. Fat is presented as yellow area. D and E, Fat and lean mass of WT and TG mice after 10-week LFD or HFD feeding (n=6 to 7). In panels B, D, and E, $^{**}P<0.01$; $^{***}P<0.001$, vs LFD within the same group. $^{\#}P<0.05$; $^{\#\#\#}P<0.001$, vs WT mice on the same diet. Data were analyzed by 2-factor ANOVA. ATRAP indicates angiotensin II type 1 receptor-associated protein; 3D micro-CT, 3-dimensional micro–computed tomography; HFD, high-fat diet; LFD, low-fat diet; TG mice, adipocyte-specific angiotensin II type 1 receptor–associated protein transgenic mice; WT mice, wild-type mice.

6B, 7A, 7B, 7E, 7F, 10A–10E, 12A, 12B, and 13C–13F). A 2-way repeated measures ANOVA was used to test for differences over time (Figures 2A, 3B, 7C, and 7D). An unpaired *t* test was used to test for differences on the same diet between 2 genotypes (Figures 3A, 8, 9A, 9B, 11, and 13B).

Results

Generation of Adipocyte-Specific ATRAP Transgenic Mice

We generated transgenic mice overexpressing ATRAP specifically in adipose tissue in vivo to investigate a functional role

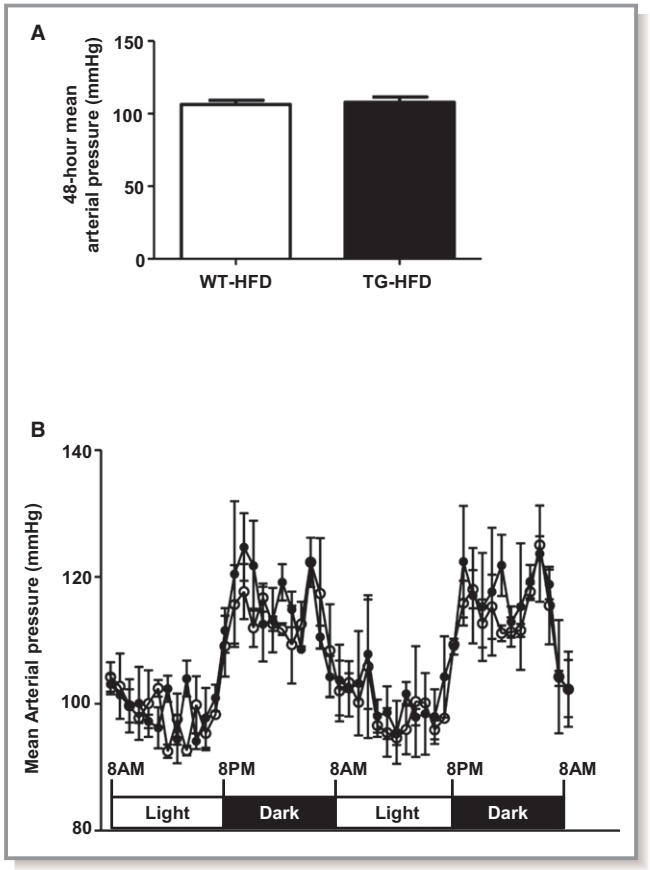

Figure 3. Blood pressure analyzed by the radiotelemetric method was comparable between WT and TG mice fed an HFD. A, The 48-hour mean arterial pressure on telemetry after 10-week HFD diet feeding (n=2 in each group). B, Diurnal mean arterial pressure profiles analyzed by the radiotelemetric method in WT and TG mice fed an HFD (n=2 in each group). ○, WT mice fed an HFD; ●, TG mice fed an HFD. A, Data were analyzed by unpaired *t* test. B, Data were analyzed by 2-way repeated measures ANOVA. HFD indicates high-fat diet; TG mice, adipocyte-specific angiotensin II type 1 receptor–associated protein transgenic mice; WT mice, wild-type mice.

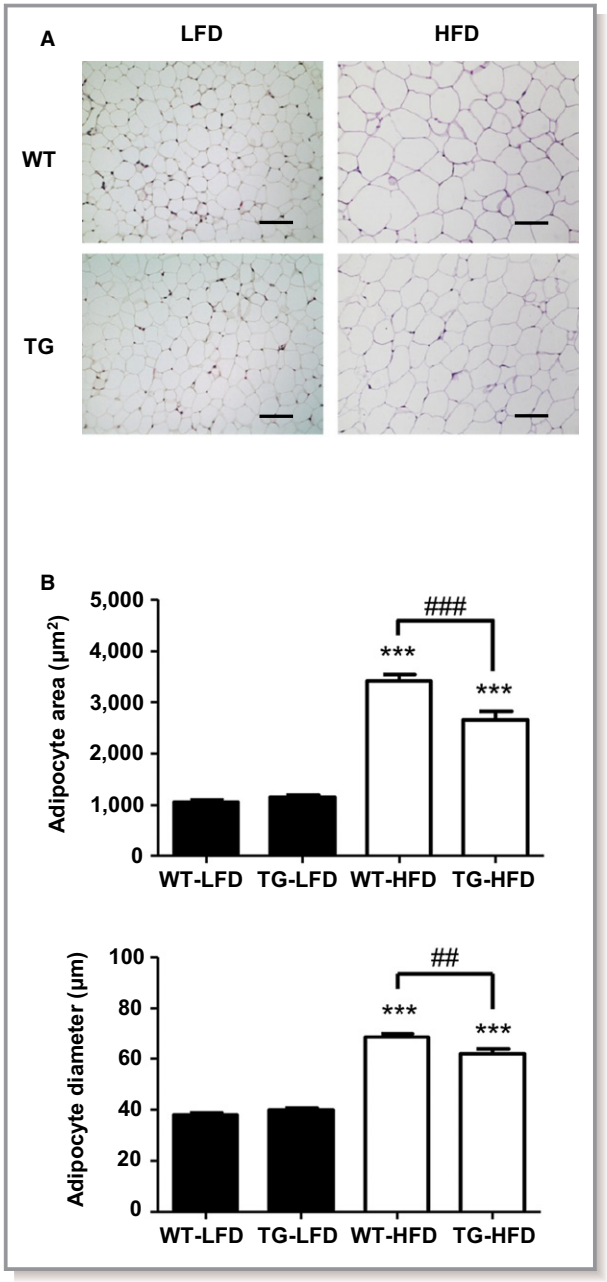

Figure 4. Adipose ATRAP enhancement prevents the adipocyte hypertrophy induced by HFD feeding. A, Representative pictures of adipocyte cell size in WAT from WT and TG mice after 10-week LFD or HFD feeding. Original magnification, ×200. Scale bar=100 μm. B, Adipocyte area and diameter of WT and TG mice after 10-week LFD or HFD feeding (n=6 to 7). $^{***}P<0.001$, vs LFD within the same group. $^{\#\#}P<0.01$, $^{\#\#\#}P<0.001$, vs WT mice on the same diet. Data were analyzed by 2-factor ANOVA. ATRAP indicates angiotensin II type 1 receptor–associated protein; HFD, high-fat diet; LFD, low-fat diet; TG mice, adipocyte-specific ATRAP transgenic mice; WT mice, wild-type mice.

of adipose ATRAP. The transgenic mice harboring the 5.4-kb adiponectin promoter fragment linked upstream of the hemagglutinin-tagged ATRAP cDNA expressed the ATRAP mRNA in adipose tissue ≈10-fold higher than in the WT mice, whereas the ATRAP mRNA expression levels in other tissues were comparable between the 2 genotypes (Figure 1B). In addition, Western blot analysis also revealed a remarkable increase of ATRAP protein level in adipose tissue from transgenic mice (Figure 1C). The 5.4-kb adiponectin promoter fragment is reportedly the most effective cassette for conveying the adipocyte-specific expression of target genes, whereas the adipocyte protein 2 (aP2) promoter has been used mainly to intend adipose tissue-dominant gene expression, but this is accompanied by substantial expression in tissues other than adipose tissue.[12] By employing the 5.4-kb adiponectin promoter cassette, we were able to more accurately investigate the functional role of ATRAP in adipose tissue.

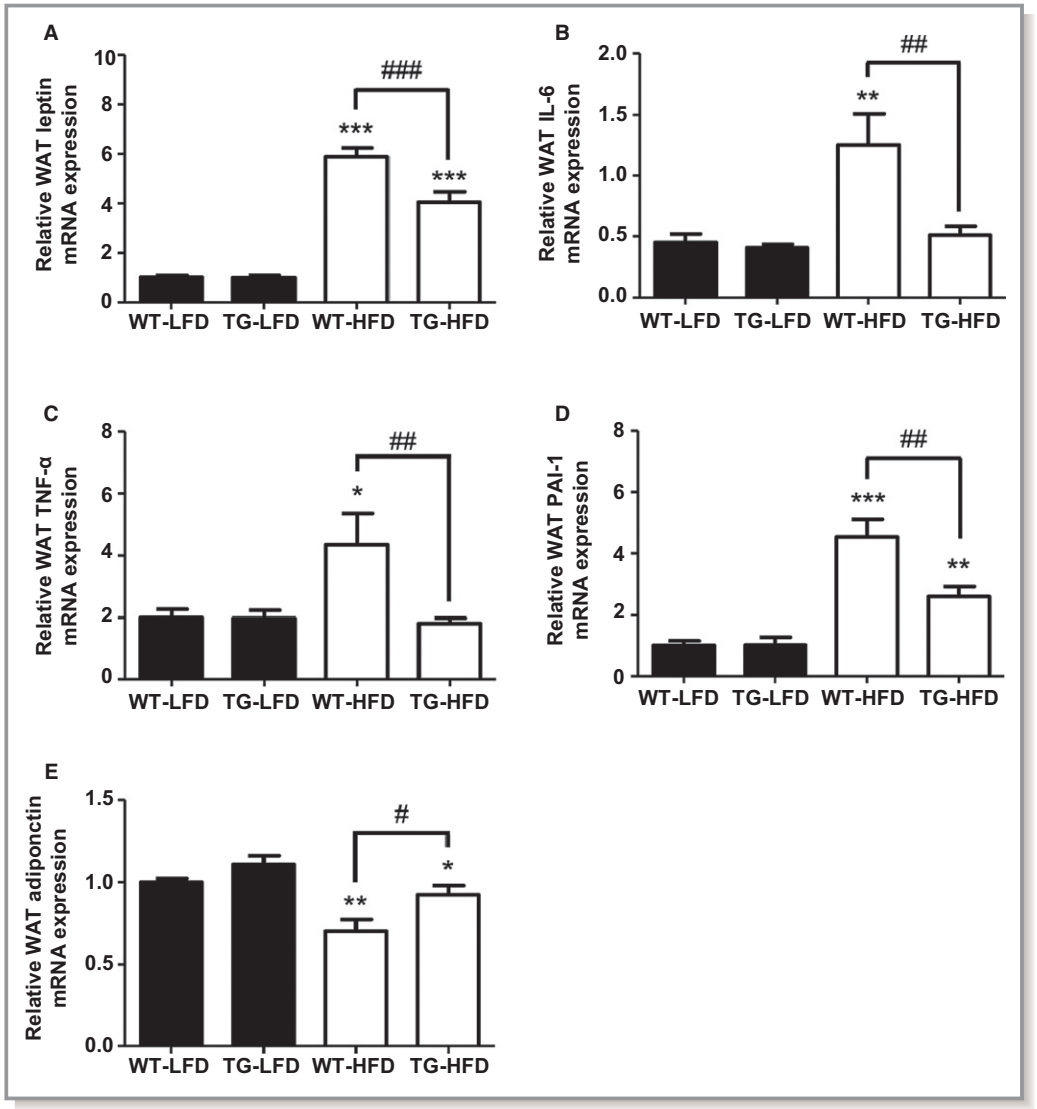

Figure 5. Adipose ATRAP enhancement improves the adipokine dysregulation induced by HFD feeding. A through E, mRNA expression of adipokines (leptin, IL-6, TNF-α, PAI-1, and adiponectin) in WAT from WT and TG mice after 10-week LFD or HFD feeding (n=6 to 7). **P*<0.05, ***P*<0.01, ****P*<0.001, vs LFD within the same group. $^{\#}P$<0.05, $^{\#\#}P$<0.01, $^{\#\#\#}P$<0.001, vs WT mice on the same diet. Data were analyzed by 2-factor ANOVA. ATRAP indicates angiotensin II type 1 receptor–associated protein; HFD, high-fat diet; IL-6, interleukin 6; LFD, low-fat diet; PAI-1, plasminogen activator inhibitor 1; TG mice, adipocyte-specific ATRAP transgenic mice; TNF-α, tumor necrosis factor α; WAT, epididymal white adipose tissue; WT mice, wild-type mice.

Adipose ATRAP Enhancement Prevents HFD-Induced Visceral Obesity

Transgenic mice fed an LFD displayed no evident anatomical abnormality or alteration in physiological parameters (Table 1). When mice were fed an HFD for 10 weeks, the increase in body weight in the transgenic mice was significantly attenuated compared with the WT mice (Figure 2A and 2B), despite the fact that their cumulative food intake were comparable between the 2 genotypes (Table 1). The results of 3-dimensional micro-CT scan analysis showed the decreased fat mass as well as the increased lean mass in transgenic mice fed an HFD compared with WT mice fed an HFD, indicating that the transgenic mice were prevented from the HFD-induced increase in adiposity (Table 1, Figure 2C through 2E). In addition, compared with WT mice, the HFD-induced increase in adipocyte cell size in WAT was significantly attenuated in transgenic mice, despite comparable adipocyte cell size in WT and transgenic mice on an LFD (Figure 4A and 4B). Systolic blood pressure and heart rates measured by the tail-cuff method in each genotype were comparable when fed an LFD and were similarly increased by

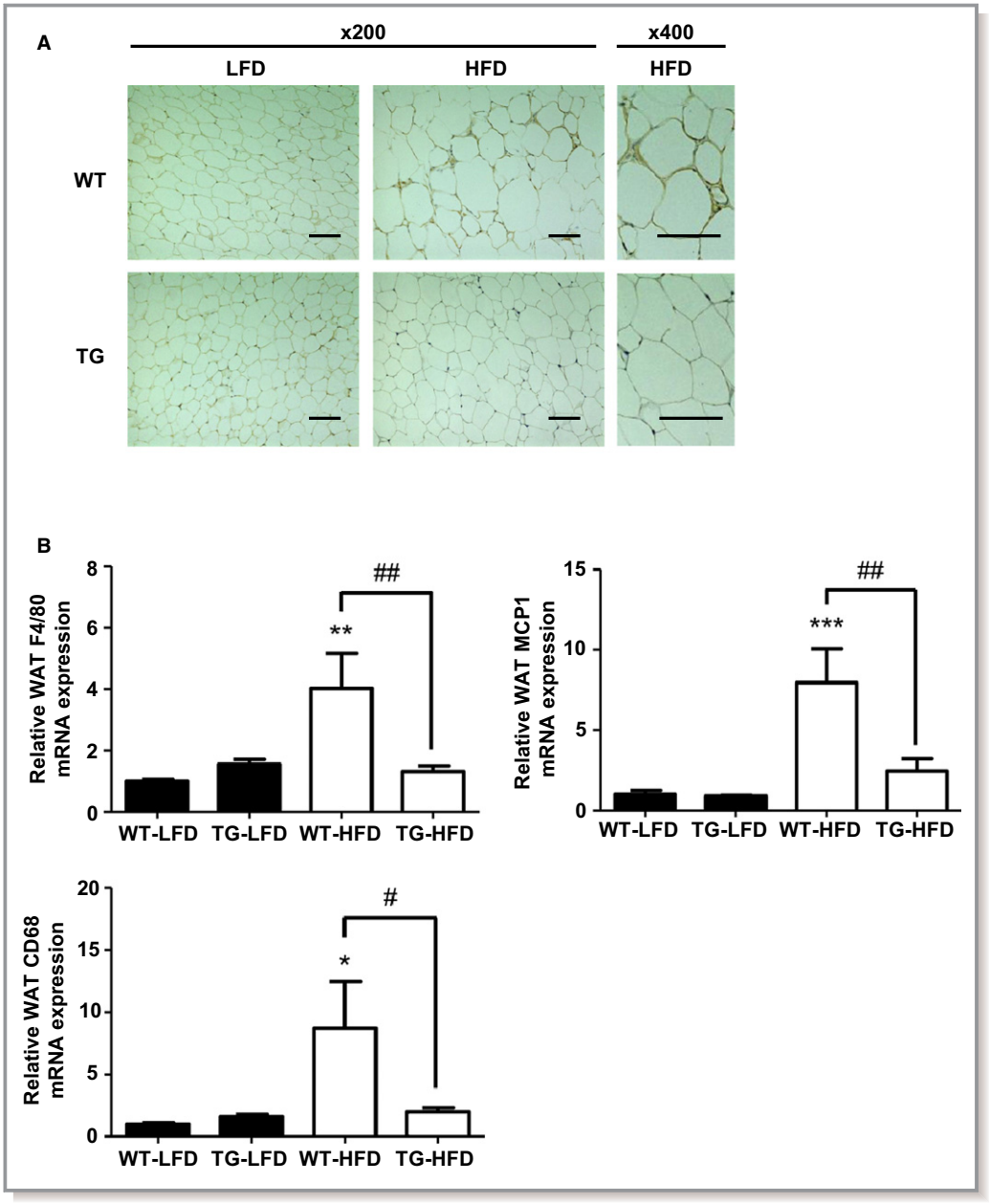

Figure 6. Adipose ATRAP enhancement attenuates the macrophage infiltration induced by HFD feeding. A, Representative pictures of WAT sections stained with the anti-F4/80 antibody. Original magnification, ×200 or ×400. Scale bar=100 μm. B, mRNA expressions of F4/80, MCP1, and CD68 in WAT from WT and TG mice after 10-week LFD or HFD feeding (n=6 to 7). $^{*}P<0.05$, $^{**}P<0.01$, $^{***}P<0.001$, vs LFD within the same group. $^{\#}P<0.05$, $^{\#\#}P<0.01$, vs WT mice on the same diet. Data were analyzed by 2-factor ANOVA. ATRAP indicates angiotensin II type 1 receptor–associated protein; HFD, high-fat diet; LFD, low-fat diet; TG mice adipocyte-specific ATRAP transgenic mice; WAT, epididymal white adipose tissue; WT mice, wild-type mice.

HFD feeding (Table 1). We further examined the difference in blood pressure between the 2 genotypes using an intra-arterial catheter telemetry system. As shown in Figure 3, mean arterial pressure in each genotype was comparable when fed an HFD (WT-HFD versus transgenic-HFD, 106.3±1.2 mm Hg versus 107.8±1.3 mm Hg, 2-way repeated measures ANOVA F=0.1148; P=0.7670).

Adipose ATRAP Enhancement Improves the Adipokine Dysregulation and Macrophage Infiltration Induced by HFD Feeding

Next, we investigated the function of visceral adipose tissue as an endocrine organ releasing adipokines in each genotype fed either an LFD or HFD. Although the mRNA

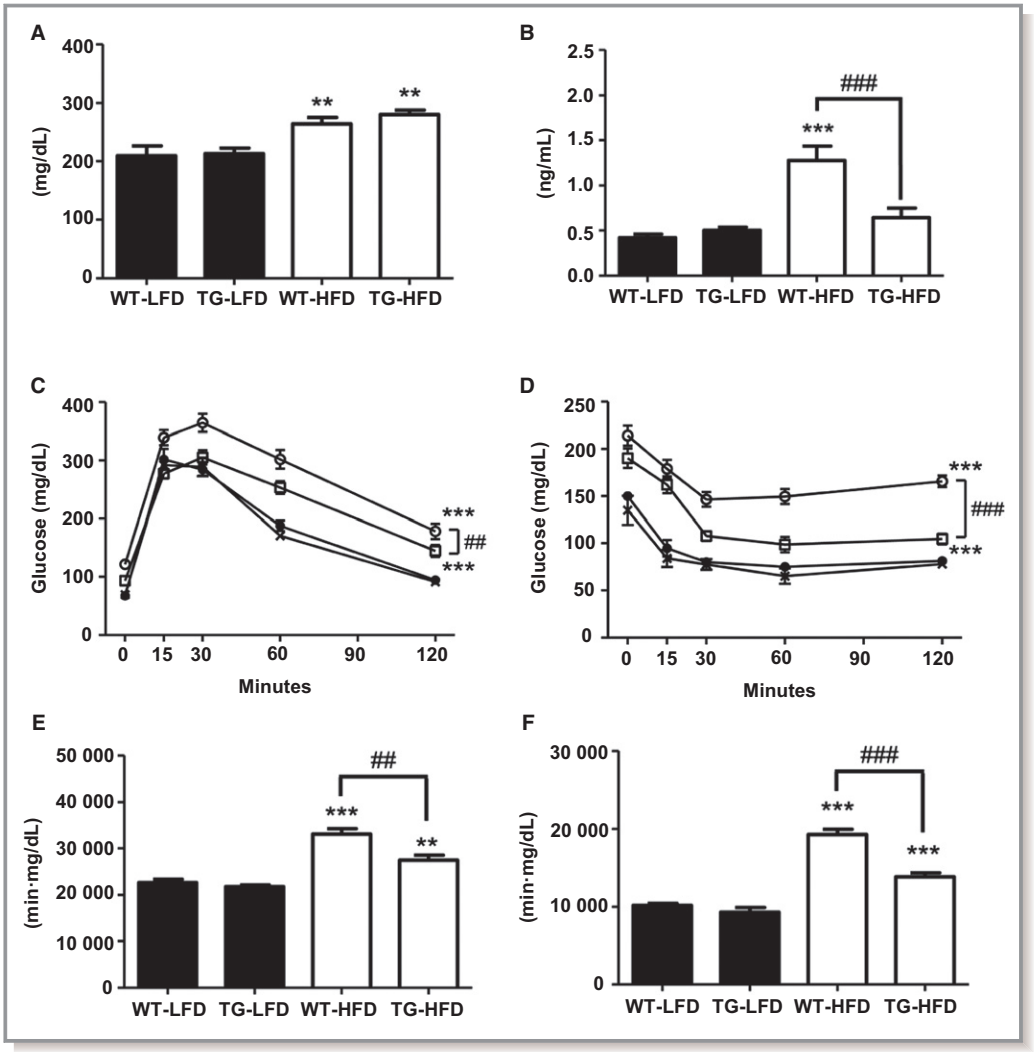

Figure 7. Adipose ATRAP enhancement improved insulin resistance induced by HFD feeding. A and B, Nonfasting blood glucose and plasma insulin concentrations in WT and TG mice after 10-week LFD or HFD feeding (n=6 to 10). C and D, The GTT and ITT in the WT and TG mice after 10-week LFD or HFD feeding (n=5 to 7). ●, WT mice fed an LFD; ×, TG mice fed an LFD; ○, WT mice fed an HFD; □, TG mice fed an HFD. E and F, The AUC of GTT and ITT in WT and TG mice after 10-week LFD or HFD feeding (n=5 to 7). A, B, E, and F, $^{**}P<0.01$, $^{***}P<0.001$, vs LFD within the same group. $^{\#\#}P<0.01$, $^{\#\#\#}P<0.001$, vs WT mice on the same diet. Data were analyzed by 2-factor ANOVA. C and D, $^{***}P<0.001$, vs LFD within the same group. $^{\#\#}P<0.01$, $^{\#\#\#}P<0.001$, vs WT mice on the same diet. Data were analyzed by 2-way repeated measures ANOVA. ATRAP indicates angiotensin II type 1 receptor–associated protein; AUC, area under curve; GTT, glucose tolerance test; HFD, high-fat diet; ITT, insulin tolerance test; LFD, low-fat diet; TG mice, adipocyte-specific ATRAP transgenic mice; WT mice, wild-type mice.

expression of adipokines in WAT was not different between the 2 mouse groups fed an LFD, the increased mRNA expression of leptin, interleukin 6, tumor necrosis factor α, and plasminogen activator inhibitor 1 was significantly attenuated in transgenic mice fed an HFD compared with WT mice fed an HFD (Figure 5A through 5D). In addition, the HFD-induced decrease in adiponectin mRNA expression was significantly attenuated in transgenic mice compared with WT mice (Figure 5E). Furthermore, the result of immunohistochemical analysis showed that the increase in HFD-induced macrophage infiltration in WAT, one of the main causes of low-grade inflammation in adipose tissue, was markedly attenuated in the transgenic compared with WT mice (Figure 6A). The increased mRNA expression in WAT of F4/80, MCP1, and CD68, markers of macrophage infiltration, were also eliminated in transgenic mice fed an HFD compared with WT mice fed an HFD (Figure 6B).

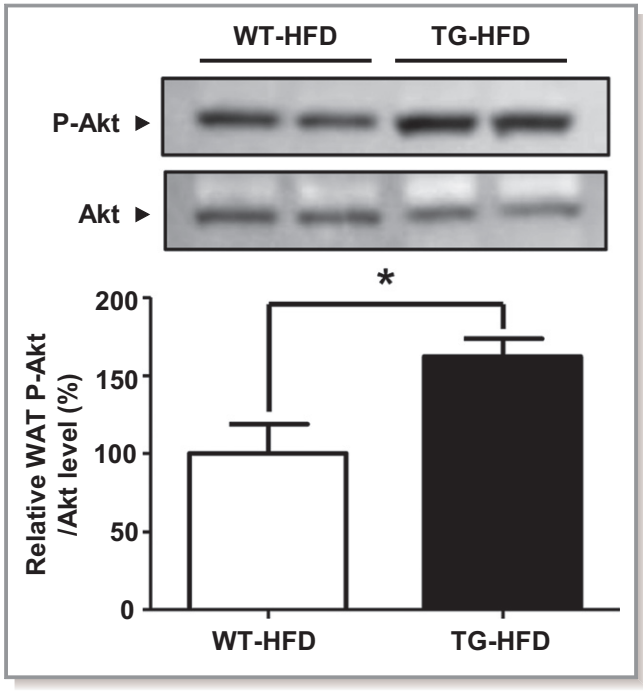

Figure 8. The level of phospho-Akt protein in WAT is increased in TG mice fed an HFD. Representative Western blots and quantitative analysis of phosphor-Akt and Akt protein levels in WAT from WT and TG mice after 10-week HFD feeding (n=5 to 6). **P*<0.05, vs WT mice on the same diet. Data were analyzed by unpaired *t* test. HFD indicates high-fat diet; TG mice, adipocyte-specific angiotensin II type 1 receptor–associated protein transgenic mice; WAT, epididymal white adipose tissue; WT mice, wild-type mice.

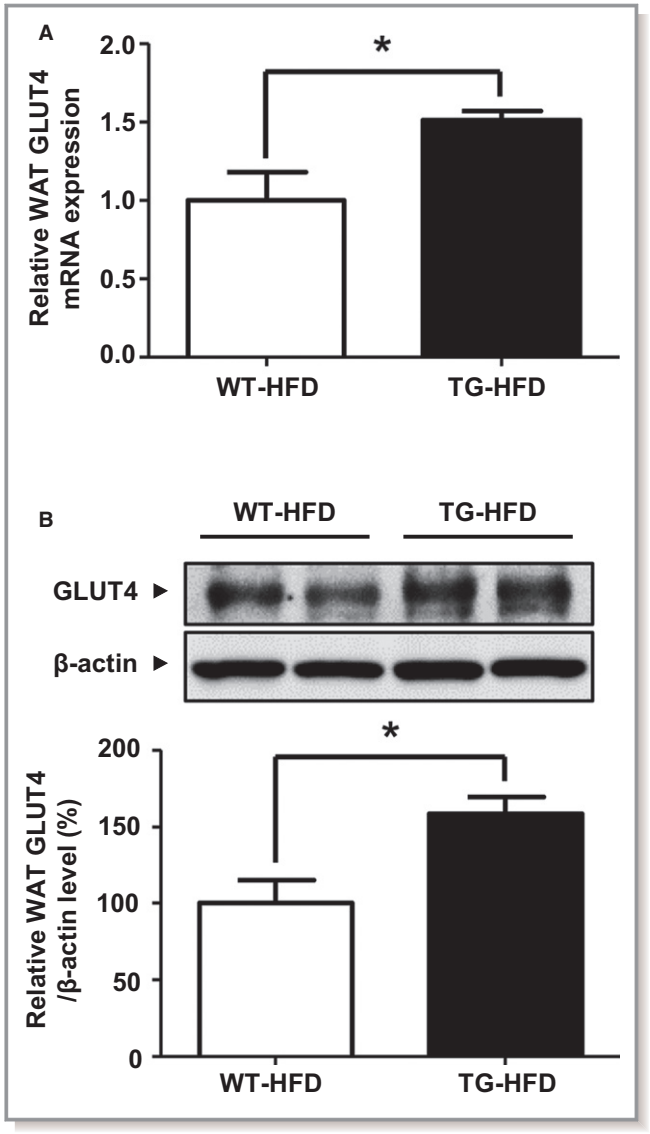

Figure 9. The expression of GLUT4 in WAT is increased in TG mice fed an HFD. A, mRNA expression of GLUT4 in WAT from WT and TG mice after 10-week HFD feeding (n=6 to 9). B, Representative Western blots and quantitative analysis of GLUT4 protein level in WAT from WT and TG mice after 10-week HFD feeding (n=6 to 7). A and B, **P*<0.05, vs WT mice on the same diet. Data were analyzed by unpaired *t* test. GLUT4 indicates glucose transporter type 4; HFD, high fat diet; TG mice, adipocyte-specific ATRAP transgenic mice; WAT, epididymal white adipose tissue; WT mice, wild-type mice.

Adipose ATRAP Enhancement Ameliorates the Insulin Resistance Induced by HFD Feeding

The evident improvement of adipose function in transgenic mice fed an HFD prompted us to examine whether diet-induced insulin resistance would be improved in transgenic mice compared with WT mice. First, we compared the blood glucose and plasma insulin concentrations between WT and transgenic mice in the fed state. Although the blood glucose concentration was comparable between the genotypes fed either an LFD or an HFD, the HFD-induced increase in the plasma insulin concentration was significantly attenuated in the transgenic mice compared with WT mice (Figure 7A and 7B). Next, to further examine the effects of adipose-specific ATRAP enhancement on insulin resistance, we performed glucose and insulin tolerance tests, which reflect the glucose tolerance and insulin sensitivity, respectively. There were no significant differences in glucose and insulin tolerance tests between WT and transgenic mice fed an LFD (Figure 7C through 7F); however, the HFD-induced exacerbation of glucose intolerance and insulin resistance was significantly improved in transgenic mice compared with WT mice (Figure 7C through 7F). To confirm the direct evidence of improved insulin resistance in transgenic mice fed an HFD, we also examined the protein level of phospho-Akt in the WAT. The protein level of phospho-Akt in WAT was significantly elevated in transgenic mice fed an HFD compared with WT mice fed an HFD (Figure 8).

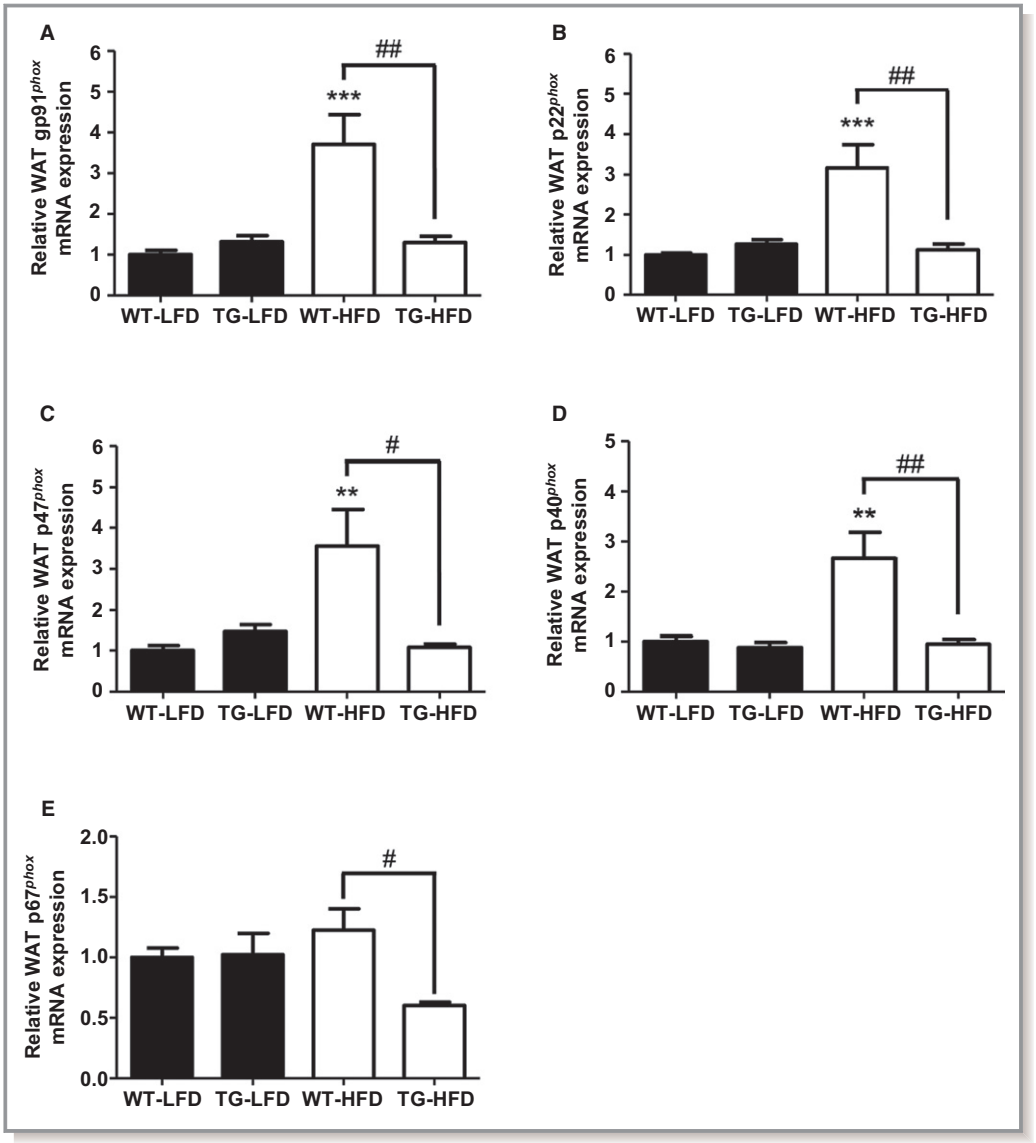

Figure 10. Adipose ATRAP enhancement ameliorates the increased mRNA expression of NADPH oxidases in WAT induced by HFD feeding. A through E, mRNA expression of NADPH oxidases in WAT from WT and TG mice after 10-week LFD or HFD feeding (n=6 to 10). $^{**}P<0.01$, $^{***}P<0.001$, vs LFD within the same group. $^{\#}P<0.05$, $^{\#\#}P<0.01$, vs WT mice on the same diet. Data were analyzed by 2-factor ANOVA. ATRAP indicates angiotensin II type 1 receptor–associated protein; HFD, high-fat diet; LFD, low-fat diet; TG mice, adipocyte-specific ATRAP transgenic mice; WAT, epididymal white adipose tissue; WT mice, wild-type mice.

WAT GLUT4 Expression in Transgenic Mice Fed an HFD Is Elevated Along With the Attenuation of NADPH Oxidase and p38 MAPK Expression

We examined the expression of adipose GLUT4, a glucose transporter isoform, to investigate the mechanism of the amelioration of insulin resistance in transgenic mice fed an HFD. The GLUT4 expression levels in WAT (Figure 9A, mRNA expression; Figure 9B, protein expression) were significantly elevated in transgenic mice compared with WT mice on an HFD. To investigate a possible mechanism involved in the elevation of WAT GLUT4 expression in transgenic mice on an HFD, we examined NADPH oxidase expression in WAT from transgenic and WT mice. NADPH oxidase–derived reactive oxygen species function as important intracellular second messengers to downregulate adipose GLUT4 expression.[5] As shown in Figure 10, the HFD-induced increase in NADPH oxidase expression in WAT was markedly ameliorated in transgenic mice compared with WT mice. We further examined the protein level of MAPK in the WAT, as the downstream signaling pathway of the AT1R. The level of phospho-p38 MAPK protein in WAT was significantly attenuated in

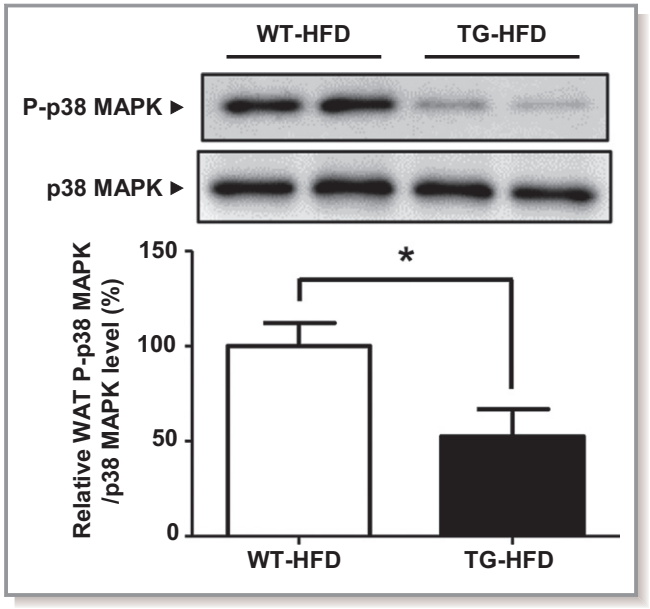

Figure 11. The level of phosho-p38 MAPK in WAT is decreased in TG mice fed an HFD. Representative Western blots and quantitative analysis of phospho-p38 MAPK and p38 MAPK protein levels in WAT from WT and TG mice after 10-week HFD feeding (n=5 to 8). **P*<0.05, vs WT mice on the same diet. Data were analyzed by unpaired *t* test. HFD indicates high fat diet; MAPK, mitogen-activated protein kinase; TG mice, adipocyte-specific angiotensin II type 1 receptor–associated protein transgenic mice; WAT, epididymal white adipose tissue; WT mice, wild-type mice.

transgenic mice compared with WT mice on an HFD (Figure 11). These results indicate that the amelioration of diet-induced oxidative stress via suppression of overactivated adipose tissue AT1R signaling contributes to the maintenance of adipose GLUT4 expression, which results in the amelioration of diet-induced insulin resistance in these transgenic mice.

Adipose ATRAP Enhancement Has No Evident Effects on the Function of BAT and Liver

Because the ATRAP expression in BAT was also enhanced in transgenic mice (Figure 1B and 1C), we examined the uncoupling protein-1 (UCP-1) and peroxisome proliferator-activated receptor gamma coactivator 1-α (PGC1-α) mRNA expression in BAT, as the markers of mitochondrial thermogenesis and biogenesis, respectively. The UCP-1 and PGC1-α mRNA expression in BAT were comparable between the 2 genotypes on an LFD and an HFD (Figure 12A and 12B). These results suggest that ATRAP enhancement in BAT may have no evident effects on its function. To elucidate the effect of liver on insulin resistance in mice fed an HFD, we also investigated the phenotypic change in liver. Although modest liver steatosis was recognized in mice fed an HFD compared with mice fed an LFD, the nonalcoholic fatty liver disease score was comparable between the 2 genotypes on an HFD (Figure 13A and 13B).

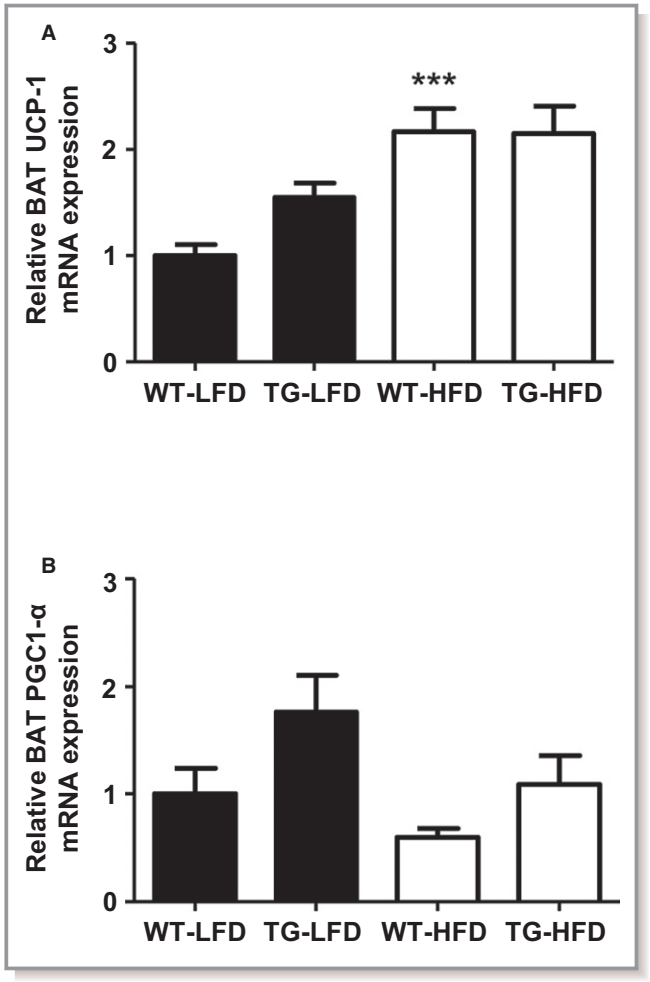

Figure 12. Adipose ATRAP enhancement does not affect the function of BAT. A and B, mRNA expressions of UCP-1 and PGC1-α in BAT from WT and TG mice after 10-week LFD or HFD feeding (n=6 to 7). ****P*<0.001, vs LFD within the same group. Data were analyzed by 2-factor ANOVA. ATRAP indicates angiotensin II type 1 receptor–associated protein; BAT, interscapular brown adipose tissue; HFD, high-fat diet; LFD, PGC1-α, peroxisome proliferator-activated receptor gamma coactivator 1-α; low-fat diet; TG, adipocyte-specific ATRAP transgenic mice; UCP-1, uncoupling protein-1; WT mice, wild-type mice.

Furthermore, the mRNA expressions of glucose-metabolism markers (glucose transporter 2 and phosphoenolpyruvate carboxykinase 1) and lipid-metabolism markers (peroxisome proliferator-activated receptor-α and sterol regulatory element-binding protein-1c) in liver was comparable between the 2 genotypes on an LFD and an HFD (Figure 13C through 13F). These results suggest that ATRAP enhancement in adipose tissue may have no evident effects on the function of liver.

Discussion

In this study, we demonstrated that adipocyte-specific ATRAP enhancement exerted the following effects. First, HFD-

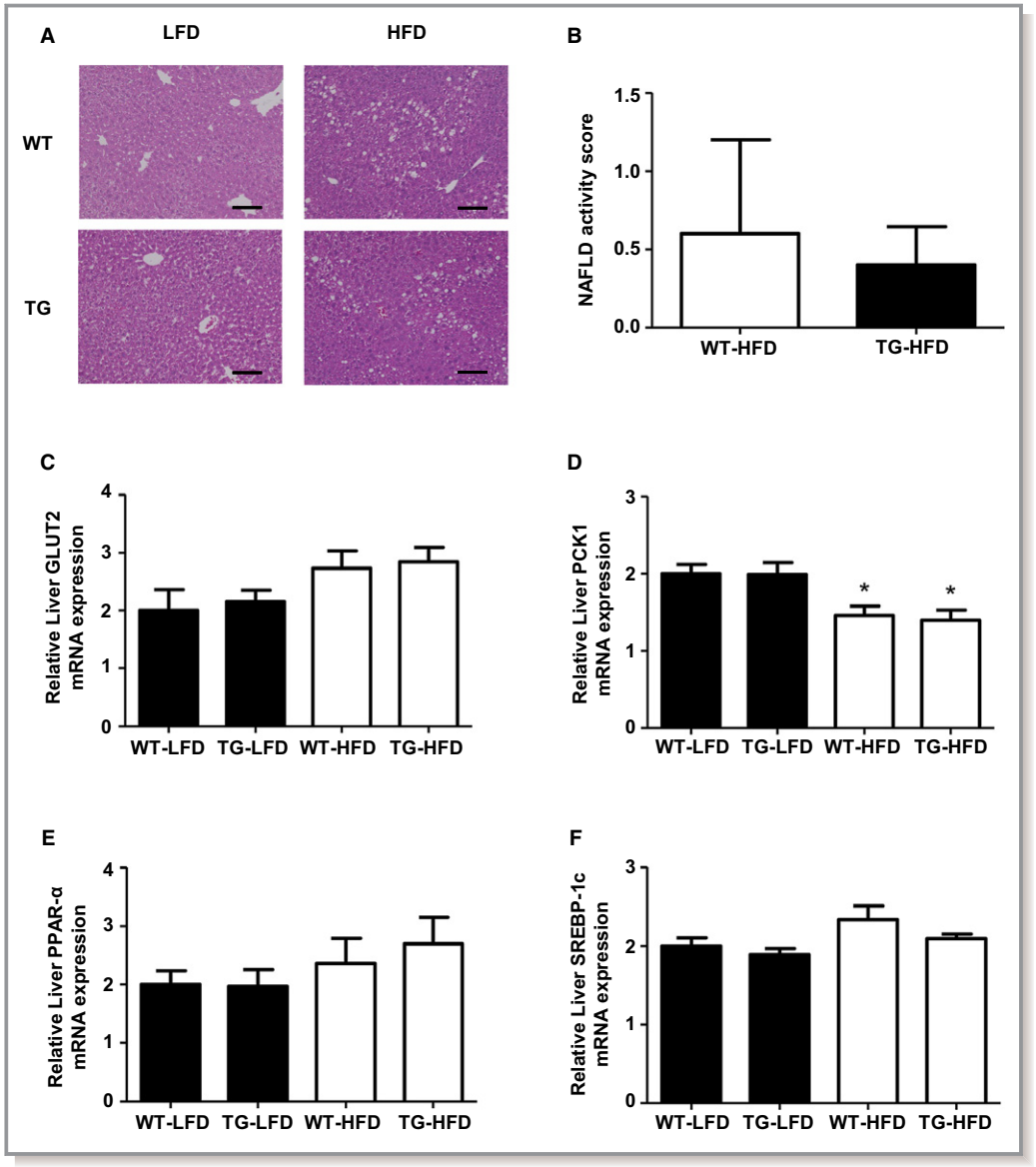

Figure 13. Adipose ATRAP enhancement does not affect the function of liver. A, Representative pictures of liver sections from WT and TG mice after 10-week LFD or HFD feeding. Original magnification, ×200. Scale bar=100 μm. B, The NAFLD activity score of liver from WT and TG mice after 10-week HFD feeding (n=5). C through F, mRNA expressions of GLUT2, PCK1, PPAR-α, and SREBP-1c in liver from WT and TG mice after 10-week LFD or HFD feeding (n=5 to 7). B, Data were analyzed by unpaired t test. C through F, **P*<0.05, vs LFD within the same group. Data were analyzed by 2-factor ANOVA. ATRAP indicates angiotensin II type 1 receptor–associated protein; GLUT2, glucose transporter 2; HFD, high-fat diet; LFD, low-fat diet; NAFLD, nonalcoholic fatty liver disease; PCK1, phosphoenolpyruvate carboxykinase 1; PPAR-α, peroxisome proliferator-activated receptor-α; SREBP-1c, sterol regulatory element-binding protein-1c; TG, adipocyte-specific ATRAP transgenic mice; WT mice, wild-type mice.

induced weight gain, adiposity, and adipocyte hypertrophy were significantly attenuated, whereas the food intake was comparable between the 2 genotypes. Second, HFD-induced adipokine dysregulation and macrophage infiltration were markedly improved. Third, the exacerbated glucose tolerance and insulin sensitivity induced by an HFD were significantly improved along with the significant increase of adipose phospho-Akt protein level. Fourth, adipose GLUT4 expression was significantly elevated concomitant with the attenuation of the adipose NADPH oxidase expression and phospho-p38 MAPK protein level under HFD feeding.

It is noteworthy that adipocyte-specific ATRAP enhancement did not result in any evident alteration in physiological function, including adipose tissue morphology, when mice

Table 2. NAFLD Activity Score

Item	Definition	Score
Steatosis	<5%	0
	5–33%	1
	>33% to 66%	2
	>66%	3
Lobular inflammation	No foci	0
	<2 foci/×200 field	1
	2–4 foci/×200 field	2
	>4 foci/×200 field	3
Hepatocyte ballooning	None	0
	Few balloon cells	1
	Many cells/prominent ballooning	2

NAFLD indicates nonalcoholic fatty liver disease.

were fed an LFD. This finding is consistent with our previous studies demonstrating that the change in ATRAP expression did not affect physiological function or organ morphology at baseline in other types of ATRAP transgenic and deficient mice.[11,13–15,19,21] In contrast, adipocyte-specific AT1R deficiency promoted striking adipocyte hypertrophy under baseline conditions on LFD feeding and failed to improve HFD-induced visceral obesity and insulin resistance.[22] Consistent with this, severe hypotension and abnormal renal morphology and function at baseline were caused by a systemic deficiency of renin, angiotensinogen, and AT1R, respectively.[23–25] These results indicate that "physiological" AT1R signaling is essential for maintaining organ homeostasis, and a "complete" blockade of AT1R receptor signaling may be very harmful in certain circumstances.

In contrast to the results of adipocyte-specific AT1R deficiency, although adipocyte-specific ATRAP enhancement did not alter the adipose tissue morphology under baseline conditions on an LFD, the HFD-induced visceral obesity and insulin resistance were remarkably ameliorated, concomitant with improvement in adipose function and inflammation. Consequently, we suggest that adipose ATRAP exerts preventive effects on diet-induced visceral obesity and insulin resistance via a functionally selective inhibition of AT1R that preserves physiological AT1R signaling without any evident harmful effects.

In the development of visceral obesity, adipocyte hypertrophy typically induces low-grade adipose inflammation and macrophage infiltration, and this phenomenon contributes to adipokine dysregulation, which is characterized by the upregulation of proinflammatory adipokines and downregulation of anti-inflammatory adipokines.[3] We demonstrated that adipocyte-specific ATRAP enhancement markedly inhibited HFD-induced adipose macrophage infiltration, NADPH oxidase expression, and adipokine dysregulation concomitant with attenuation of adipocyte hypertrophy. The mechanisms of how adipose ATRAP enhancement attenuates adipocyte hypertrophy are unclear at present, but a possible explanation is the increase of energy expenditure in transgenic mice. Because there was no difference in the food intake between the 2 genotypes, we consider that the increase of systemic energy expenditure may be elicited by adipose ATRAP enhancement and cause the prevention of HFD-induced body weight gain and adipocyte hypertrophy in transgenic mice. Although the beneficial effects of adipose ATRAP enhancement may be elicited by the attenuation of adipocyte hypertrophy, further studies will be required to elucidate the underlying mechanisms by which adipose ATRAP regulates adipocyte differentiation.

Adipocyte-specific ATRAP enhancement improved HFD-mediated glucose intolerance and insulin resistance. GLUT4 plays a main role in glucose uptake from the blood into muscle as well as adipose tissue, and the dysfunction of this transporter becomes a potent trigger of insulin resistance.[26] In terms of the regulation of GLUT4 in adipocyte, the overactivation of AT1R signaling reportedly promotes the production of reactive oxygen species by increasing NADPH oxidases, and this in turn contributes to the reduction of GLUT4 expression and the impairment of GLUT4 translocation.[5] In the present study, adipose GLUT4 expression was significantly elevated concomitant with the attenuation of adipose NADPH oxidases in transgenic mice compared with WT mice on an HFD. Thus, the HFD-resistant maintenance of adipose GLUT4 function via the attenuated induction of NADPH oxidase by adipose ATRAP enhancement is the mechanism responsible for the amelioration of HFD-induced insulin resistance in these transgenic mice. This hypothesis is confirmed by the result that adipose phospho-Akt protein level was significantly elevated in transgenic mice on an HFD.

To confirm the reduction of renin–angiotensin system–AT1R signaling in adipose tissue, we examined the phosphorylation level of p38-MAPK in WAT, as the downstream signaling pathway of the AT1R. Several previous studies have reported that, in particular, the phosphorylation of p38 MAPK is elicited mainly in cardiovascular cells by overactivation of the renin–angiotensin system.[27–29] As expected, the level of adipose phospho-p38 MAPK was significantly attenuated in transgenic mice fed an HFD, and this result suggests that adipose ATRAP enhancement may be able to suppress the overactivation of adipose AT1R signaling.

The present study has several limitations. First, although adipocyte-specific ATRAP enhancement has preventive effects against diet-induced visceral obesity and insulin resistance, HFD feeding is not a factor that directly stimulates AT1R

signaling. Therefore it is necessary to further investigate the role of adipose ATRAP in angiotensin-dependent insulin resistance using angiotensin II stimulation in vivo.[30] Second, it should also be examined whether similarly preventative effects may be obtained without any harmful effects when the degree of adipose ATRAP enhancement is changed. Third, locomotor activity and resting metabolic rate data, which estimate energy expenditure, are lacking in this study. Because the food intake was comparable between the 2 genotypes, we consider that these parameters would be enhanced in transgenic mice. Further studies will be needed to elucidate this issue.

Nevertheless, this study shows that adipocyte-specific ATRAP enhancement exerts protective effects against diet-induced visceral obesity and insulin resistance, and these effects are concomitant with an improvement in adipose function and inflammation. In addition, these beneficial effects are evidently independent of any harmful effects. The data obtained from this study suggest that adipose tissue ATRAP is a promising therapeutic target for the treatment of visceral obesity.

Acknowledgments

We acknowledge the help of Dr Philipp E. Scherer (The University of Texas Southwestern Medical Center), who provided us with the 5.4-kb fragment of adiponectin promoter.

Sources of Funding

This work was supported by a grants-in-aid of The Cardiovascular Research Fund, Tokyo, Japan, and by Grant-in-Aid for Young Scientists (B) from the Japan Society for the Promotion of Science (JSPS). This work was also supported by a Health and Labor Sciences Research grant, by Grants-in-Aid for Scientific Research from the JSPS, and by grants from SENSHIN Medical Research, Banyu Life Science Foundation International, and Salt Science Research Foundation (No. 1428).

Disclosures

Tamura received research grant or honoraria from Takeda, Daiichi-Sankyo, Kyowa-hakko Kirin, Shionogi, Dainippon-Sumitomo, Novartis, Chu-gai, Mochida, MSD, Tanabe Mitsubishi, Boehringer Ingelheim, Astellas, Pfizer, AstraZeneca and Sanofi. Umemura received research grant or honoraria from Pfizer, Daiichi-Sankyo, Boehringer Ingelheim, AstraZeneca, Astellas, Kowa, Shionogi, Novartis, MSD, Dainippon-Sumitomo, Torii, Takeda, Tanabe Mitsubishi, Kyowa-hakko Kirin, Byer, Ohtsuka, Chugai, Mochida, Sanwa-kagaku and Teijin. The remaining authors declare no conflict of interest.

References

1. Ng M, Fleming T, Robinson M, Thomson B, Graetz N, Margono C, Mullany EC, Biryukov S, Abbafati C, Abera SF, Abraham JP, Abu-Rmeileh NM, Achoki T, AlBuhairan FS, Alemu ZA, Alfonso R, Ali MK, Ali R, Guzman NA, Ammar W, Anwari P, Banerjee A, Barquera S, Basu S, Bennett DA, Bhutta Z, Blore J, Cabral N, Nonato IC, Chang JC, Chowdhury R, Courville KJ, Criqui MH, Cundiff DK, Dabhadkar KC, Dandona L, Davis A, Dayama A, Dharmaratne SD, Ding EL, Durrani AM, Esteghamati A, Farzadfar F, Fay DF, Feigin VL, Flaxman A, Forouzanfar MH, Goto A, Green MA, Gupta R, Hafezi-Nejad N, Hankey GJ, Harewood HC, Havmoeller R, Hay S, Hernandez L, Husseini A, Idrisov BT, Ikeda N, Islami F, Jahangir E, Jassal SK, Jee SH, Jeffreys M, Jonas JB, Kabagambe EK, Khalifa SE, Kengne AP, Khader YS, Khang YH, Kim D, Kimokoti RW, Kinge JM, Kokubo Y, Kosen S, Kwan G, Lai T, Leinsalu M, Li Y, Liang X, Liu S, Logroscino G, Lotufo PA, Lu Y, Ma J, Mainoo NK, Mensah GA, Merriman TR, Mokdad AH, Moschandreas J, Naghavi M, Naheed A, Nand D, Narayan KM, Nelson EL, Neuhouser ML, Nisar MI, Ohkubo T, Oti SO, Pedroza A, Prabhakaran D, Roy N, Sampson U, Seo H, Sepanlou SG, Shibuya K, Shiri R, Shiue I, Singh GM, Singh JA, Skirbekk V, Stapelberg NJ, Sturua L, Sykes BL, Tobias M, Tran BX, Trasande L, Toyoshima H, van de Vijver S, Vasankari TJ, Veerman JL, Velasquez-Melendez G, Vlassov VV, Vollset SE, Vos T, Wang C, Wang X, Weiderpass E, Werdecker A, Wright JL, Yang YC, Yatsuya H, Yoon J, Yoon SJ, Zhao Y, Zhou M, Zhu S, Lopez AD, Murray CJ, Gakidou E. Global, regional, and national prevalence of overweight and obesity in children and adults during 1980–2013: a systematic analysis for the Global Burden of Disease Study 2013. *Lancet*. 2014;384:766–781.

2. NCD Risk Factor Collaboration (NCD-RisC). Trends in adult body-mass index in 200 countries from 1975 to 2014: a pooled analysis of 1698 population-based measurement studies with 19.2 million participants. *Lancet*. 2016; 387:1377–1396.

3. Fuster JJ, Ouchi N, Gokce N, Walsh K. Obesity-induced changes in adipose tissue microenvironment and their impact on cardiovascular disease. *Circ Res*. 2016;118:1786–1807.

4. Littlejohn NK, Grobe JL. Opposing tissue-specific roles of angiotensin in the pathogenesis of obesity, and implications for obesity-related hypertension. *Am J Physiol Regul Integr Comp Physiol*. 2015;309:R1463–R1473.

5. Favre GA, Esnault VL, Van Obberghen E. Modulation of glucose metabolism by the renin-angiotensin-aldosterone system. *Am J Physiol Endocrinol Metab*. 2015;308:E435–E449.

6. DREAM Trial Investigators, Bosch J, Yusuf S, Gerstein HC, Pogue J, Sheridan P, Dagenais G, Diaz R, Avezum A, Lanas F, Probstfield J, Fodor G, Holman RR. Effect of ramipril on the incidence of diabetes. *N Engl J Med*. 2006;355:1551–1562.

7. NAVIGATOR Study Group, McMurray JJ, Holman RR, Haffner SM, Bethel MA, Holzhauer B, Hua TA, Belenkov Y, Boolell M, Buse JB, Buckley BM, Chacra AR, Chiang FT, Charbonnel B, Chow CC, Davies MJ, Deedwania P, Diem P, Einhorn D, Fonseca V, Fulcher GR, Gaciong Z, Gaztambide S, Giles T, Horton E, Ilkova H, Jenssen T, Kahn SE, Krum H, Laakso M, Leiter LA, Levitt NS, Mareev V, Martinez F, Masson C, Mazzone T, Meaney E, Nesto R, Pan C, Prager R, Raptis SA, Rutten GE, Sandstroem H, Schaper F, Scheen A, Schmitz O, Sinay I, Soska V, Stender S, Tamás G, Tognoni G, Tuomilehto J, Villamil AS, Vozár J, Califf RM. Effect of valsartan on the incidence of diabetes and cardiovascular events. *N Engl J Med*. 2010;362:1477–1490.

8. Tamura K, Tanaka Y, Tsurumi Y, Azuma K, Shigenaga A, Wakui H, Masuda S, Matsuda M. The role of angiotensin AT1 receptor-associated protein in renin-angiotensin system regulation and function. *Curr Hypertens Rep*. 2007;9:121–127.

9. Tamura K, Wakui H, Maeda A, Dejima T, Ohsawa M, Azushima K, Kanaoka T, Haku S, Uneda K, Masuda S, Azuma K, Shigenaga A, Koide Y, Tsurumi-Ikeya Y, Matsuda M, Toya Y, Tokita Y, Yamashita A, Umemura S. The physiology and pathophysiology of a novel angiotensin receptor-binding protein ATRAP/Agtrap. *Curr Pharm Des*. 2013;19:3043–3048.

10. Tamura K, Wakui H, Azushima K, Uneda K, Haku S, Kobayashi R, Ohki K, Haruhara K, Kinguchi S, Matsuda M, Yamashita A, Umemura S. Angiotensin II type 1 receptor binding molecule ATRAP as a possible modulator of renal sodium handling and blood pressure in pathophysiology. *Curr Med Chem*. 2015;22:3210–3216.

11. Maeda A, Tamura K, Wakui H, Dejima T, Ohsawa M, Azushima K, Kanaoka T, Uneda K, Matsuda M, Yamashita A, Miyazaki N, Yatsu K, Hirawa N, Toya Y, Umemura S. Angiotensin receptor-binding protein ATRAP/Agtrap inhibits metabolic dysfunction with visceral obesity. *J Am Heart Assoc*. 2013;2: e000312. DOI: 10.1161/JAHA.113.000312.

12. Wang ZV, Deng Y, Wang QA, Sun K, Scherer PE. Identification and characterization of a promoter cassette conferring adipocyte-specific gene expression. *Endocrinology*. 2010;151:2933–2939.

13. Wakui H, Tamura K, Tanaka Y, Matsuda M, Bai Y, Dejima T, Masuda S, Shigenaga A, Maeda A, Mogi M, Ichihara N, Kobayashi Y, Hirawa N, Ishigami T, Toya Y, Yabana M, Horiuchi M, Minamisawa S, Umemura S. Cardiac-specific

activation of angiotensin II type 1 receptor-associated protein completely suppresses cardiac hypertrophy in chronic angiotensin II-infused mice. *Hypertension*. 2010;55:1157–1164.

14. Wakui H, Tamura K, Masuda S, Tsurumi-Ikeya Y, Fujita M, Maeda A, Ohsawa M, Azushima K, Uneda K, Matsuda M, Kitamura K, Uchida S, Toya Y, Kobori H, Nagahama K, Yamashita A, Umemura S. Enhanced angiotensin receptor-associated protein in renal tubule suppresses angiotensin-dependent hypertension. *Hypertension*. 2013;61:1203–1210.
15. Wakui H, Dejima T, Tamura K, Uneda K, Azuma K, Maeda A, Ohsawa M, Kanaoka T, Azushima K, Kobayashi R, Matsuda M, Yamashita A, Umemura S. Activation of angiotensin II type 1 receptor-associated protein exerts an inhibitory effect on vascular hypertrophy and oxidative stress in angiotensin II-mediated hypertension. *Cardiovasc Res*. 2013;100:511–519.
16. Imajo K, Fujita K, Yoneda M, Nozaki Y, Ogawa Y, Shinohara Y, Kato S, Mawatari H, Shibata W, Kitani H, Ikejima K, Kirikoshi H, Nakajima N, Saito S, Maeyama S, Watanabe S, Wada K, Nakajima A. Hyperresponsivity to low-dose endotoxin during progression to nonalcoholic steatohepatitis is regulated by leptin-mediated signaling. *Cell Metab*. 2012;16:44–54.
17. Shigenaga A, Tamura K, Wakui H, Masuda S, Azuma K, Tsurumi-Ikeya Y, Ozawa M, Mogi M, Matsuda M, Uchino K, Kimura K, Horiuchi M, Umemura S. Effect of olmesartan on tissue expression balance between angiotensin II receptor and its inhibitory binding molecule. *Hypertension*. 2008;52:672–678.
18. Azushima K, Tamura K, Wakui H, Maeda A, Ohsawa M, Uneda K, Kobayashi R, Kanaoka T, Dejima T, Fujikawa T, Yamashita A, Toya Y, Umemura S. Bofu-tsu-shosan, an oriental herbal medicine, exerts a combinatorial favorable metabolic modulation including antihypertensive effect on a mouse model of human metabolic disorders with visceral obesity. *PLoS One*. 2013;8:e75560.
19. Wakui H, Uneda K, Tamura K, Ohsawa M, Azushima K, Kobayashi R, Ohki K, Dejima T, Kanaoka T, Tsurumi-Ikeya Y, Matsuda M, Haruhara K, Nishiyama A, Yabana M, Fujikawa T, Yamashita A, Umemura S. Renal tubule angiotensin II type 1 receptor-associated protein promotes natriuresis and inhibits salt-sensitive blood pressure elevation. *J Am Heart Assoc*. 2015;4:e001594. DOI: 10.1161/JAHA.114.001594.
20. Oshikawa J, Otsu K, Toya Y, Tsunematsu T, Hankins R, Kawabe J, Minamisawa S, Umemura S, Hagiwara Y, Ishikawa Y. Insulin resistance in skeletal muscles of caveolin-3-null mice. *Proc Natl Acad Sci USA*. 2004;101:12670–12675.
21. Ohsawa M, Tamura K, Wakui H, Maeda A, Dejima T, Kanaoka T, Azushima K, Uneda K, Tsurumi-Ikeya Y, Kobayashi R, Matsuda M, Uchida S, Toya Y, Kobori H, Nishiyama A, Yamashita A, Ishikawa Y, Umemura S. Deletion of the angiotensin II type 1 receptor-associated protein enhances renal sodium reabsorption and exacerbates angiotensin II-mediated hypertension. *Kidney Int*. 2014;86:570–581.
22. Putnam K, Batifoulier-Yiannikouris F, Bharadwaj KG, Lewis E, Karounos M, Daugherty A, Cassis LA. Deficiency of angiotensin type 1a receptors in adipocytes reduces differentiation and promotes hypertrophy of adipocytes in lean mice. *Endocrinology*. 2012;153:4677–4686.
23. Yanai K, Saito T, Kakinuma Y, Kon Y, Hirota K, Taniguchi-Yanai K, Nishijo N, Shigematsu Y, Horiguchi H, Kasuya Y, Sugiyama F, Yagami Ki, Murakami K, Fukamizu A. Renin-dependent cardiovascular functions and renin-independent blood-brain barrier functions revealed by renin-deficient mice. *J Biol Chem*. 2000;275:5–8.
24. Niimura F, Labosky PA, Kakuchi J, Okubo S, Yoshida H, Oikawa T, Ichiki T, Naftilan AJ, Fogo A, Inagami T. Gene targeting in mice reveals a requirement for angiotensin in the development and maintenance of kidney morphology and growth factor regulation. *J Clin Invest*. 1995;96:2947–2954.
25. Oliverio MI, Delnomdedieu M, Best CF, Li P, Morris M, Callahan MF, Johnson GA, Smithies O, Coffman TM. Abnormal water metabolism in mice lacking the type 1A receptor for ANG II. *Am J Physiol Renal Physiol*. 2000;278:F75–F82.
26. Govers R. Molecular mechanisms of GLUT4 regulation in adipocytes. *Diabetes Metab*. 2014;40:400–410.
27. Griendling KK, Ushio-Fukai M. Reactive oxygen species as mediators of angiotensin II signaling. *Regul Pept*. 2000;91:21–27.
28. Liu Z, Cao W. p38 mitogen-activated protein kinase: a critical node linking insulin resistance and cardiovascular diseases in type 2 diabetes mellitus. *Endocr Metab Immune Disord Drug Targets*. 2009;9:38–46.
29. Palomeque J, Delbridge L, Petroff MV. Angiotensin II: a regulator of cardiomyocyte function and survival. *Front Biosci*. 2009;14:5118–5133.
30. Takeda M, Yamamoto K, Takemura Y, Takeshita H, Hongyo K, Kawai T, Hanasaki-Yamamoto H, Oguro R, Takami Y, Tatara Y, Takeya Y, Sugimoto K, Kamide K, Ohishi M, Rakugi H. Loss of ACE2 exaggerates high-calorie diet-induced insulin resistance by reduction of GLUT4 in mice. *Diabetes*. 2013;62:223–233.